AIAA AVIATION Forum
5-9 June 2017, Denver, Colorado
35th AIAA Applied Aerodynamics Conference

10.2514/6.2017-3261

Multi-Fidelity Uncertainty Analysis in CFD using Hierarchical Kriging

Pramudita Satria Palar* and Koji Shimoyama†
Tohoku University, Sendai 980-8577, Japan

Multi-fidelity uncertainty analysis method is a potential technique to speed up the process of uncertainty quantification (UQ) when expensive computational simulations are involved. In this paper, we investigate the capability of the hierarchical Kriging (HK) method for multi-fidelity uncertainty analysis, especially for applications in computational fluid dynamics (CFD). Besides the conventional HK method, we also enhanced the HK method by utilizing polynomial chaos expansion (PCE) and the ensemble of Kriging and PCE as the low-fidelity surrogate model. We also extend the formulation of HK so to allow the use of extra polynomial terms to further enhance the approximation capability of HK. The MF framework was firstly demonstrated on the multi-fidelity Branin and Ishigami function. Computational studies on two CFD test problems were performed and the results were compared with Kriging, PCE, and multi-fidelity PCE. In the light of these results, we found that using the ensemble of PCE and Kriging as the low-fidelity surrogate model is a better and more robust approach to deal with various problems in UQ instead of using just one type of surrogate model for HK. The HK framework is also more efficient than that of the multi-fidelity PCE method which relies on a simple correction function. The results of the common research model and RAE 2822 problems reveal the remarkable efficiency of HK for UQ in inviscid CFD-based problems with multi-fidelity simulations. On the RAE 2822 problem, the use of first order polynomial scaling function is necessary in order to create a more accurate HK approximation relative to the single-fidelity surrogate model.

I. Introduction

The presence of uncertainties is inevitable in the analysis of real-world engineering/physical systems. Failure to understand the effect of uncertainty propagation might result in a functional failure or a poor performance of an engineering system. Thus, it is important that the effect of uncertainties should be considered in the analysis, design, or even optimization process. Uncertainty analysis can be simply done by applying a Monte Carlo simulation (MCS) strategy, which is very simple and also robust to the curse-of-dimensionality issue. However, when one is faced with expensive simulations, the use of MCS is not practically useful anymore due to the limited availability of the computational budget. To cope with this problem, one common way to handle uncertainty quantification (UQ) problem is to employ surrogate model (or metamodel) to approximate the relationship between the random input and the random output with a cheap analytical expression. Among several popular surrogate models in the literature are Kriging,[1] polynomial regression,[2] radial basis function (RBF),[3] polynomial chaos expansion,[4,5] and support vector regression.[6] Most of these surrogate models are widely employed to speed up the process of engineering design optimization. For UQ, only a handful of them have already been studied and used.

UQ in aerodynamics typically involves a computational fluid dynamics (CFD) code coupled with a code for an uncertainty assessment in order to analyze the stochastic performance of aerodynamic bodies. Uncertainties could come from the disturbance in the flight condition, which is probabilistic in nature and can be described with the probability theory (called the aleatoric uncertainty). On the other hand, if uncertainties come from the modeling of the problem (called the model form/epistemic uncertainty), they are non-probabilistic and have to be described using other approaches such as the Dempster-Shafer theory.[7] The

*Postdoctoral Fellow, Institute of Fluid Science, 2-1-1 Katahira, Aoba-ku
†Associate Professor, Institute of Fluid Science, 2-1-1 Katahira, Aoba-ku.

uncertainty assessment can be done in either an intrusive or a non-intrusive way, with the latter is easier to be implemented since it does not involve the modification of the CFD code itself. UQ of aerodynamic bodies is a particular importance when the presence of uncertainties greatly affects the aerodynamic performance. UQ is also important in the process of aerodynamic robust optimization,[8–10] in which the objective is to find optimum aerodynamic designs that are robust to the perturbation in the design/flight condition.

Although in practice any surrogate model can be used for UQ, PCE and Kriging are the most frequent types of surrogate models used in UQ, especially the former which relies on the orthogonal polynomial expansion to approximate the random function. There are several reasons why PCE is popular in the UQ literature, among them are the smoothness, theoretical convergence, and ease of implementation. Another field where PCE recently becomes popular is sensitivity analysis (SA), in which the goal is to identify and quantify the contribution of each term of the random input to the random output. In fact, the PCE method is a convenience technique for SA since the Sobol sensitivity index can be directly computed from information of the PCE coefficients.[11,12] Based on how the PCE coefficients are computed, the PCE method can be classified into *spectral-projection*[4] and *regression-based* methods.[5] PCE has been successfully applied to UQ in various fluid dynamics and aerodynamics cases.[13–17] In this paper, the regression-based method, where the PCE coefficients are calculated using the unstructured sampling and the least squares technique, was used. Specifically, the sparse PCE with least-angle-regression (LARS) was employed.[18]

Other than PCE is the Kriging-based method.[1] The most widely used form of Kriging is ordinary Kriging (OK) which employs a constant trend instead of a non-constant trend as in universal Kriging. Since Kriging offers a direct estimation of the prediction error, an adaptive sampling technique that explores this prediction error is straightforward to use.[19,20] Furthermore, if gradient information is available, it can be utilized to enhance the quality of the approximation.[21,22] Some applications of Kriging in real-world CFD-based problems are the UQ of a fluid-structure interaction case[23] and a transonic airfoil.[24] The attractiveness of Kriging is mainly located on its high generalization capability and the direct possibility for adaptive sampling. However, Kriging is not suitable for high-dimensional UQ problems due to the difficulty in training the hyperparameters and the curse-of-dimensionality. Nonetheless, in low-dimensionality UQ problems, one can expect a competitive performance of Kriging when compared to the PCE.[25]

A recent trend in UQ/SA is the incorporation of multi-fidelity (MF) simulations to accelerate the overall computation process. When the access to low-fidelity (LF) simulations such as simulations with different governing equation, mesh accuracy, or convergence criteria is available, they can be utilized together with high-fidelity (HF) simulations to improve the accuracy within the MF framework. In the PCE literature, MF-PCE methods have been studied and investigated to speed up the UQ and the aerodynamic robust optimization process.[26–28] The multi-fidelity Kriging method, which is co-Kriging in this respect,[29] has been applied to the UQ of a sailing yacht hull[30] and for global SA.[31]

An alternative version of MF Kriging is the hierarchical Kriging (HK)[32] method that treats the LF function as the trend for the HF function. This reduces the complexity of the HK method compared to co-Kriging. HK has been successfully applied in the context of MF optimization and can produce a better accuracy and a better optimized solution compared to co-Kriging.[32] Another merit of HK is that there is no need for the HF sample set to be the subset of LF sample set, as in the case of co-Kriging. In spite of its potential, the HK method has not been extensively studied for UQ. Study on the capabilities of HK for MF UQ is important in order to extend its use toward problem solving in UQ. Moreover, there is a potential for the improvement of the HK method, such as replacing the low-fidelity surrogate model with other surrogate model types. This has motivated us to study and enhance the HK method in order to efficiently solve UQ problems. In this paper, we studied some of these potentials together with computational studies on some algebraic and aerodynamic test problems. The enhancement of the HK method proposed by us is to use PCE and the ensemble of PCE and OK as an alternative LF surrogate model. Furthermore, we extended the HK formulation so that it is able to include a polynomial scaling function in order to improve the flexibility of HK.

The paper is organized as follows: in Section II we details the original formulation of HK. The explanation of the implementation of HK for UQ is given in Section III. Section IV presents the application to three examples: the Ishigami function, the common research model (CRM) problem in the Euler flow, and the inviscid RAE 2822 case. Finally, the paper is concluded and the future work is given in Section V.

II. Hierarchical Kriging

HK is a multi-fidelity approximation method based on Kriging that uses the LF function as the trend for the HF function.[32] This is a different methodology compared to correction-based MF methods and co-Kriging that need the modeling of the correction function.[29] As shown by Han and Görtz,[32] HK has a simpler formulation and can produce a better solution than that of co-Kriging when applied in the optimization context. The HK method itself has not been extensively studied for UQ purpose, in spite of its potential to do such thing. The explanation of HK in its original paper treats the variables as decision variables $\boldsymbol{x}$. In this paper, without loss of generality, we replaced $\boldsymbol{x}$ with random variables $\boldsymbol{\xi} = \{\xi_1, \ldots, \xi_r\}$, where r is the number of random variables, in the following formulation of HK since our interest is to solve UQ problems. The following explanation of HK is based on the original paper of HK by Han and Görtz.[32]

The HK surrogate model is built by firstly preparing the experimental design (ED) for the HF and the LF function, denoted as $\boldsymbol{\mathcal{X}}_h = \{\boldsymbol{\xi}^{(1)}, \ldots, \boldsymbol{\xi}^{(n_h)}\}$ and $\boldsymbol{\mathcal{X}}_l = \{\boldsymbol{\xi}^{(1)}, \ldots, \boldsymbol{\xi}^{(n_l)}\}$, respectively, where $n_l > n_h$. The output of the HF and the LF function is denoted as a vector $\boldsymbol{y}_h = \{y^{(1)}, \ldots, y^{(n_h)}\}$ and $\boldsymbol{y}_l = \{y^{(1)}, \ldots, y^{(n_l)}\}$, respectively.

The high-fidelity function corresponds to the original HK method is formulated by

$$Y(\boldsymbol{\xi}) = \beta_0 \hat{f}_{lf}(\boldsymbol{\xi}) + Z(\boldsymbol{\xi}). \tag{1}$$

The HK method can be expanded into its more generalized form by adding polynomial terms $\boldsymbol{\psi}(\boldsymbol{\xi}) = \{\psi_0(\boldsymbol{\xi}), \ldots, \psi_{P-1}(\boldsymbol{\xi})\}^T$ to the scaling function, where P is the polynomial basis size. The generalized form of HK is written as

$$Y(\boldsymbol{\xi}) = \boldsymbol{\psi}(\boldsymbol{\xi})^T \boldsymbol{\beta} \hat{f}_{lf}(\boldsymbol{\xi}) + Z(\boldsymbol{\xi}), \tag{2}$$

where $\boldsymbol{\beta} = \{\beta_0, \ldots, \beta_{P-1}\}^T$ are the corresponding polynomial coefficients. This formulation is similar to the variable-fidelity Kriging formula explained in Han and Görtz[33] but differs in a sense that the generalized HK formula still treats the LF function as the trend, where the polynomial function has a role to further refine the scaling between the LF and the HF function. We then use this generalized form of HK for the following detail explanation of the HK method.

One can see that in Eq. 2 the constant trend in OK is replaced by $\boldsymbol{\psi}(\boldsymbol{\xi})^T \boldsymbol{\beta} \hat{f}_{lf}(\boldsymbol{\xi})$ term, which is the LF surrogate model $\hat{f}_{lf}(\boldsymbol{\xi})$ multiplied by the scaling function, serving as the trend for the stationary random process $Z(.)$. This is the core of HK that differs it from other MF Kriging methodologies. Instead of modeling the cross-correlation between the HF and the LF function as in co-Kriging,[29] HK treats the LF surrogate model as the trend for the HF function. We can see that this formulation means that HK allows more freedom in the sampling method that made it not necessary to set the HF sample set as the subset of the LF sample set.

Kriging assumes that a slight difference between the location of two points also means that the difference between their respective objective is small. To model this assumption, Kriging assumes that there is a statistical correlation between two sets of random variables. Although various forms of correlation exist, in this paper we assume that the correlation is in the form of the Gaussian exponential function, reads as

$$R(\boldsymbol{\theta}, \boldsymbol{\xi}, \boldsymbol{\xi}') = \prod_{k=1}^{r} \exp\left(-\theta_k |\xi_k - \xi_k'|^{p_k}\right), \tag{3}$$

where $\boldsymbol{\theta} = (\theta_1, \ldots, \theta_r)$ are the hyperparameters to be tuned, which are the distance weight in this case. Although the value of p_k can be tuned, in this paper we fixed the p_k value to 2.

After some derivation, the HK predictor then reads as

$$\hat{f}(\boldsymbol{\xi}) = \boldsymbol{\psi}(\boldsymbol{\xi})^T \boldsymbol{\beta} \hat{f}_{lf}(\boldsymbol{\xi}) + \boldsymbol{r}(\boldsymbol{\xi})^T \boldsymbol{R}^{-1} (\boldsymbol{y}_h - \boldsymbol{F}\boldsymbol{\beta}), \tag{4}$$

where

$$\boldsymbol{r} := (R(\boldsymbol{\xi}^{(i)}, \boldsymbol{\xi}))_i \in \mathbb{R}^{n_h}, \qquad \boldsymbol{R} := (\boldsymbol{R}(\boldsymbol{\xi}^{(i)}, \boldsymbol{\xi}^{(j)}))_{i,j} \in \mathbb{R}^{n_h \times n_h},$$

and $\boldsymbol{F}$ is the $n_h \times P$ matrix with the (i, j) component is $F_{i,j} = [\psi_j(\boldsymbol{\xi}_h^{(i)}) \hat{f}_{lf}(\boldsymbol{\xi}_h^{(i)})]$. The mean-squared error (MSE) of the HK prediction reads as

$$MSE\{\hat{f}(\boldsymbol{\xi})\} = \sigma^2\{1.0 - \boldsymbol{r}^T\boldsymbol{R}^{-1}\boldsymbol{r} + [\boldsymbol{r}^T\boldsymbol{R}^{-1}\boldsymbol{F} - \{\boldsymbol{\psi}(\boldsymbol{\xi})\}\hat{f}_{lf}(\boldsymbol{\xi})](\boldsymbol{F}^T\boldsymbol{R}^{-1}\boldsymbol{F})^{-1}[\boldsymbol{r}^T\boldsymbol{R}^{-1}\boldsymbol{F} - \{\boldsymbol{\psi}(\boldsymbol{\xi})\}\hat{f}_{lf}(\boldsymbol{\xi})]^T\}. \tag{5}$$

Note that the $\{\boldsymbol{\psi}(\boldsymbol{\xi})\}\hat{f}_{lf}(\boldsymbol{\xi})$ term denotes the multiplication between a vector $\boldsymbol{\psi}(\boldsymbol{\xi})$ and a scalar $\hat{f}_{lf}(\boldsymbol{\xi})$. The hyperparameters are selected in order to maximize the likelihood function

$$L(\beta_0, \sigma^2, \boldsymbol{\theta}) = \frac{1}{\sqrt{(2\pi\sigma^2)^{n_h}|\boldsymbol{R}|}}\exp\left(-\frac{1}{2}\frac{(\boldsymbol{y}_h - \boldsymbol{F}\boldsymbol{\beta})^T\boldsymbol{R}^{-1}(\boldsymbol{y}_h - \boldsymbol{F}\boldsymbol{\beta})}{\sigma^2}\right), \tag{6}$$

with the following optimal estimates of the scaling factor and the process variance are as follows:

$$\hat{\boldsymbol{\beta}} = (\boldsymbol{F}^T\boldsymbol{R}^{-1}\boldsymbol{F})^{-1}\boldsymbol{F}^T\boldsymbol{R}^{-1}\boldsymbol{y}_h, \tag{7}$$

$$\sigma^2(\boldsymbol{\theta}, \beta_0) = \frac{1}{n_h}(\boldsymbol{y}_h - \boldsymbol{F}\boldsymbol{\beta})^T\boldsymbol{R}^{-1}(\boldsymbol{y}_h - \boldsymbol{F}\boldsymbol{\beta}). \tag{8}$$

The first step of HK is to build the LF surrogate model $\hat{f}_{lf}(\boldsymbol{\xi})$ to act as the trend function for the HF surrogate model. In the original formulation of HK, the LF surrogate model is built by using OK (hence the name hierarchical Kriging). However, this formulation also suggests that an arbitrary surrogate model can be used for the LF function. We will demonstrate in this paper that one can exploit the flexibility of the LF surrogate model to enhance the performance of HK. Nonetheless, theoretically, the best surrogate model for the LF function is no surrogate at all (direct MCS), since applying surrogate model implies the use of assumption on the LF function.

HK was originally proposed to solve expensive optimization problems. In this work, we extend the HK method so that it can solve various UQ problems when simulations with multiple-levels of fidelity are available.

III. Using Hierarchical Kriging for Uncertainty Analysis

In this paper, we studied the applicability of the HK method for UQ. Some enhancements to the HK method that we proposed and investigated are explained in this section. The enhancements include: 1) the use of PCE and the ensemble of PCE and Kriging as an alternative surrogate model for the LF function, and 2) polynomial scaling function (see Eq. 2).

III.A. Uncertainty quantification problem

Our objective is to compute the probabilistic output response $f(\boldsymbol{\xi})$ of a system when subjected to input uncertainties. Specifically, we have an interest in solving UQ cases that involve expensive computer-based simulations. For UQ, the task is to compute the mean and standard deviation of $f(\boldsymbol{\xi})$, denoted as $\mu(f(\boldsymbol{\xi}))$ and $\sigma(f(\boldsymbol{\xi}))$, respectively. Computation of statistical moments using standard MCS can be done as

$$\mu(f(\boldsymbol{\xi})) = \int_{\boldsymbol{\Omega}} f(\boldsymbol{\xi})\rho(\boldsymbol{\xi})\mathrm{d}\boldsymbol{\xi} \approx \frac{\sum_{j=1}^{n_{uq}} f(\boldsymbol{\xi}^{(j)})}{n_{uq}}, \tag{9}$$

and

$$\sigma(f(\boldsymbol{\xi})) = \int_{\boldsymbol{\Omega}} (f(\boldsymbol{\xi}) - \mu(\boldsymbol{\xi}))^2\rho(\boldsymbol{\xi})\mathrm{d}\boldsymbol{\xi} \approx \sqrt{\frac{\sum_{j=1}^{n_{uq}}(f(\boldsymbol{\xi}^{(j)}) - \mu(\boldsymbol{\xi}))^2}{n_{uq}}}. \tag{10}$$

where n_{uq} is the number of samples used for MCS, while $\boldsymbol{\Omega}$ and $\rho(\boldsymbol{\xi})$ are the domain of integration and the joint probability distribution, respectively. Surrogate model-based UQ can be done by simply changing $f(\boldsymbol{\xi})$ in the rightmost term of Eqs. 9 and 10 with the surrogate model $\hat{f}(\boldsymbol{\xi})$, which is exactly what we did in this work. If solely PCE is used to approximate statistical moments, they can be directly obtained from the PCE coefficients.[13] Here, we refer to the process of performing MCS with a surrogate model as the inexpensive MCS (IMCS).

In this paper, we enhanced the existing HK formulation by introducing PCE as an alternative LF surrogate model. We then also introduce the use of the ensemble of PCE and OK to build the LF surrogate

model. The main framework of the method is HK, while PCE and the surrogates ensemble serve as a surrogate model to approximate the response surface of the LF function. This provides more flexibility and potential enhancement in the generalization capability of the HK method, especially for UQ applications considered in this paper.

III.B. Enhancement with Polynomial Chaos Expansion

We propose the use of PCE, specifically LARS-based PCE, in this study as an alternative to approximate the LF function. Here, we only outline the general explanation of LARS-based PCE without giving too many details in the derivation and implementation. Readers are suggested to refer to the original paper[18] for the detail implementation of LARS-based PCE.

Consider an index defined by $\boldsymbol{\zeta} = \{\zeta_1, \ldots, \zeta_r\}$ where $\zeta_i = 0, 1, 2, \ldots$ and an index set $\mathcal{I}_{\mathbf{p}}$, PCE works by approximating a random function with

$$f_{lf}(\boldsymbol{\xi}) \approx \hat{f}_{PC}(\boldsymbol{\xi}) = \sum_{\boldsymbol{\zeta} \in \mathcal{I}_{\mathbf{p}}} \alpha_{\boldsymbol{\zeta}}(\boldsymbol{\xi}) \Theta_{\boldsymbol{\zeta}}(\boldsymbol{\xi}), \tag{11}$$

where $\boldsymbol{\Theta}(\boldsymbol{\xi}) = \{\Theta_0(\boldsymbol{\xi}), \ldots, \Theta_P(\boldsymbol{\xi})\}$ is the set of multi-dimensional polynomial bases as the product of one-dimensional bases. The index for polynomial expansion $\mathcal{I}_{\mathbf{p}}$ can be built by using a tensor product or a total-order expansion applied to one-dimensional bases. The key principle of sparse PCE is to find the subset of a given set of polynomial bases that yields the lowest leave-one-out cross-validation (LOOCV) error using the LARS algorithm. This eliminates the need to manually set polynomial bases whilst effectively reducing the likelihood of overfitting. Due to the use of regression to build the polynomial expansion, the size and location of sampling points can be adjusted arbitrarily in contrast to the spectral-projection based PCE.

The orthogonal polynomials Θ can take different form according to the probability distribution. As for example, Legendre and Hermite polynomials are the optimal orthogonal polynomials for a uniform and normal distribution, respectively.

III.C. Ensemble approach: combining PCE and Kriging for the low-fidelity surrogate model

Besides enhancing HK with the PCE surrogate model for the LF function, we also consider the ensemble of PCE and Kriging as the third option. We hypothesized that using a single type of surrogate model as the LF surrogate model does not mean a better approximation quality for all problems. To cope with this issue, the ensemble approach is also considered.[34] The ensemble approach for PCE and Kriging works as

$$f_{lf}(\boldsymbol{\xi}) \approx \hat{f}_{ens}(\boldsymbol{\xi}) = w_1 \hat{f}_{PC}(\boldsymbol{\xi}) + w_2 \hat{f}_{KR}(\boldsymbol{\xi}), \tag{12}$$

where $\hat{f}_{KR}$ is the prediction of the LF function based on the OK surrogate model, and w_1 and w_2 are the weight factor assigned to the PCE and OK surrogate model, respectively, under the equality constraint of $w_1 + w_2 = 1$.

Although there are various approaches to ensemble the surrogate models, here we opt for the error-based minimization ensemble scheme of Acar and Rohani.[35] This ensemble scheme was proved to be robust enough for our implementation and study in this paper. The error-based ensemble approach works by finding $\boldsymbol{w}$, which is $\boldsymbol{w} = \{w_1, w_2\}$ in our papers, by solving the minimization problem of

$$\min_{\boldsymbol{w}} \text{MSE}_{\text{WAS}} \ = \mathbb{E}\big(e^2_{\text{WAS}}(\boldsymbol{\xi}) \text{d}\boldsymbol{\xi}\big) = \mathbf{w}^T \mathbf{C} \mathbf{w}, \tag{13}$$

where $e_{\text{WAS}}(\boldsymbol{\xi}) = f(\boldsymbol{\xi}) - \hat{f}(\boldsymbol{\xi})$ is the error between the actual and the predicted response. Here, $\mathbf{C}$ is a matrix whose (i, j) value is defined as

$$c_{ij} \simeq \frac{1}{n_s} \hat{\mathbf{e}}_i^T \hat{\mathbf{e}}_j, \tag{14}$$

where n_s is the number of samples, which is $n_s = n_l$ for the LF surrogate model, and $\hat{\mathbf{e}}_i$ and $\hat{\mathbf{e}}_j$ are the vector of cross-validation (CV) errors for the surrogate model i and j, respectively (note that there are only two surrogate models considered in this paper). There exists an analytical technique to obtain $\hat{\mathbf{e}}$ calculated using LOOCV procedure for PCE and Kriging (see Blatman and Sudret[18] and Dubrule,[36] respectively), which allows a fast assessment and construction process of the ensemble of surrogate models. We used this analytical technique to obtain the LOOCV error in this paper.

III.D. Implementation

The flow of UQ using HK can be summarized as follows:

1. Generate the ED for the LF and HF surrogate models ($\boldsymbol{\mathcal{X}}_l$ and $\boldsymbol{\mathcal{X}}_h$, respectively).
2. Calculate response outputs, that is, $\boldsymbol{y}_l$ and $\boldsymbol{y}_h$.
3. Build the surrogate model $\hat{f}_{lf}$ for the LF function using $\boldsymbol{\mathcal{X}}_l$ and $\boldsymbol{y}_l$.
4. Build the HK surrogate model $\hat{f}_{hf}$ using $\boldsymbol{\mathcal{X}}_h$, $\boldsymbol{y}_h$, and $\hat{f}_{lf}(\boldsymbol{\mathcal{X}}_h)$.
5. Calculate statistical moments using IMCS, with IMCS samples $\boldsymbol{\mathcal{X}}_{IMC}$ are generated according to $\rho(\boldsymbol{\xi})$.

Firstly, the set of samples for the LF and HF surrogate models have to be generated. To generate sampling points, the use of low-discrepancy sequences or the latin hypercube sampling (LHS) with a high space-filling property are encouraged to ensure a high-quality surrogate model (note again that HF sampling points do not necessarily to be the subset of LF sampling points). If the distribution is not uniform, sampling points can be generated according to the uniform distribution and then transformed to the actual distribution. The HK surrogate model is then constructed using the generated sampling set, where IMCS is performed on the HK surrogate model to calculate statistical moments and the output probability distribution.

In the following, we firstly demonstrate this methodology on the Branin function.

III.E. Demonstration: Branin function

We firstly demonstrate the framework of uncertainty analysis using HK on the multi-fidelity Branin function.[37]

The HF Branin function is expressed as

$$f_{hf}(\boldsymbol{\xi}) = \left(\xi_2 - \frac{5.1}{4\pi^2}\xi_1^2 + \frac{5}{\pi}\xi_1 - 6\right)^2 + 10\left(1 - \frac{1}{8\pi}\right)\cos(\xi_1) + 10, \tag{15}$$

and the LF function as[37]

$$f_{lf}(\boldsymbol{\xi}) = f_{hf}(\boldsymbol{\xi}) - (A + 0.5)\left(\xi_2 - \frac{5.1}{4\pi^2}\xi_1^2 + \frac{5}{\pi}\xi_1 - 6\right)^2. \tag{16}$$

The LF function is constructed by using the A value of 0. This example also gives a demonstration of how to use HK with a non-uniform distribution, which is the normal distribution in this case. The random variables are ξ_1 and ξ_2 that are normally distributed with the mean value of 0.5 and the standard deviation of 0.05. Sampling points for HF and LF surrogate models were generated using the transformed Halton and Sobol sequence, respectively. To assess the efficiency of the generated surrogate model, the normalized mean absolute error ($NMAE$) is calculated via

$$NMAE = \frac{\frac{1}{n_v}\sum_{i=1}^{n_v}|f(\boldsymbol{\xi}^{(i)}) - \hat{f}(\boldsymbol{\xi}^{(i)})|}{\mu(f(\boldsymbol{\xi}))}, \tag{17}$$

where n_v is the size of validation samples. In this example, five types of surrogate model: OK, PCE (with LARS), and HK with OK, PCE, and the ensemble of LF surrogate models (denoted as HK-OK, HK-PC, and HK-EN, respectively) were used to approximate the true response. A constant scaling function was used here, which means that the LF function multiplied by a constant β_0 was used as the trend function. For this demonstration, n_h and n_l were set to 6 and 50, respectively, where the HF, LF, and IMCS sampling points set are shown in Fig. 1. The results are shown in Table 1 and Fig. 2.

The results show that the HK surrogate model was able to take the advantage of the abundant amount of LF samples to assist the MF approximation on the UQ of Branin function. The $NMAE$ from the OK, PCE, HK-PC, HK-OK, and HK-EN are 0.0549, 0.2102, 0.0085, 0.0088, and 0.0085, respectively. For clearer illustration, the depiction of response surfaces generated by OK, PCE, and HK, together with the high- and low-fidelity Branin function are shown in Fig. 2 (the surface generated by HK-EN is not shown since it is

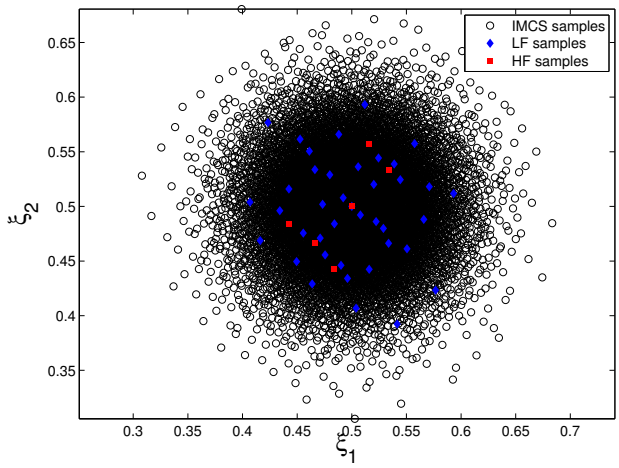

Figure 1: Samples used for the LF surrogate model (blue diamonds), HF surrogate model (red squares), and IMCS (black dots) on the Branin function

similar to the HK-PC). Boundaries shown in this figure are boundaries of vertices constructed by IMCS samples. Firstly, we can see that the difference between the LF Branin function (Fig.2b) and the HF Branin function (Fig.2a) is obvious. However, it is also visible to see that the LF Branin function can mimic the behavior of the HF function to some degree. Implementation of single-fidelity OK and PCE results in a far from accurate approximation, which in turn results in a highly inaccurate estimation of statistical moments due to the limited HF evaluations. On the other hand, we can see that all HK schemes produced more accurate approximation as it can be observed in Figs.2e and 2f which show the response surfaces of both HK schemes that closely mimic the true HF function. Moreover, although still not very close to the true values, statistical moments obtained by HK are closer to values obtained by MCS as compared to OK and PCE.

This example demonstrates the usefulness of the HK framework to perform UQ. On the next section, we explain the results of computational studies on one synthetic and two CFD-based test problems.

Method	$NMAE$	$\mu(f(\boldsymbol{\xi}))$	$\sigma(f(\boldsymbol{\xi}))$
True (MCS)	-	26.4017	7.9843
OK	0.0549	25.5363	5.8965
PCE	0.2102	24.8808	7.0207
HK-PC	0.0085	26.6144	8.2373
HK-OK	0.0088	26.6145	8.1872
HK-EN	0.0085	26.6144	8.2373

Table 1: Results from computational demonstration on the Branin problem.

IV. Computational Studies and Results

Three test problems were used as benchmark problems to investigate the performance of HK and enhanced HK: the Ishigami function, the common research model (CRM) in the Euler flow problem, and the inviscid RAE 2822 problem. Comparison with OK and PCE (with LARS) was also investigated. On CFD-based problems, we also compared the regression-based MF-PCE method[27] that utilizes LARS to select the polynomial basis.[18]

IV.A. Ishigami function

The Ishigami function[38] is a three-dimensional highly non-linear function and is a very difficult function to be approximated. To simulate the case with multi-fidelity simulations, we modified the original Ishigami function to construct its LF representation. We investigated the performance of HK with $n_h = 30$ and

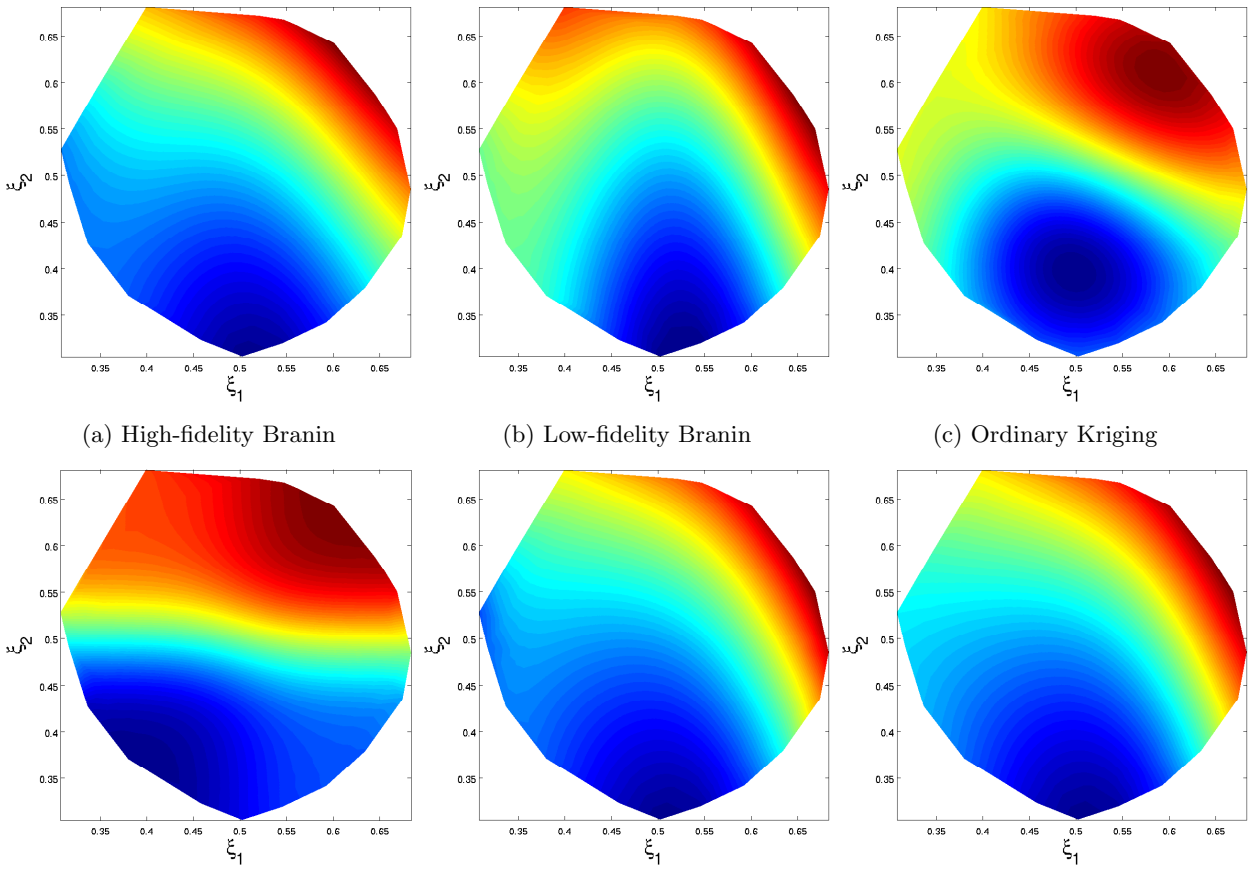

(a) High-fidelity Branin (b) Low-fidelity Branin (c) Ordinary Kriging

(d) PCE (e) Hierarchical Kriging-PCE (f) Hierarchical Kriging-OK

Figure 2: The HF function, the LF function, and generated surrogate models for the Branin function.

$n_h = 60$, with the size of the LF ED was set to three times the size of HF samples. For the Ishigami problem, we repeated the numerical experiment 50 times using 50 different set of sampling points generated by LHS. The ED for LF and HF surrogate models were generated separately since it is not necessary to set the HF sample set as the subset of the LF sample set. A constant multiplied by the LF function was used as the HK trend function for this problem. The results for the Ishigami function are shown in the form of boxplot that depicts the $NMAE$ and statistical moments obtained using 50 different sampling sets.

The HF Ishigami function is expressed as

$$f_{hf}(\boldsymbol{\xi}) = \sin(\xi_1) + 7\sin^2(\xi_2) + 0.1\xi_3^4\sin(\xi_1), \tag{18}$$

we then constructed the LF representation of the Ishigami function defined as

$$f_{lf}(\boldsymbol{\xi}) = \sin(\xi_1) + 7.3\sin^2(\xi_2) + 0.08\xi_3^4\sin(\xi_1). \tag{19}$$

where $\boldsymbol{\xi} = \{\xi_1, \xi_2, \xi_3\}$ and all random variables are uniformly distributed in the range of $[-\pi, \pi]$.

We firstly analyzed the performance of HK with a low number of HF samples (i.e., $n_h = 30, n_l = 90$). It is as expected and obvious from Fig. 3a that all HK schemes were better than OK on approximating the complex Ishigami function. However, the most notable fact here is that the performance of HK-PC outperformed HK-OK, which is the standard form of HK. Moreover, the performance of HK-EN is similar to HK-PC, which means that HK-EN successfully picked the best of surrogate models to be used as the surrogate model for the LF function. This is because when the ensemble of surrogate models was executed, the contribution of PCE was larger than that of the OK as indicated by the significantly higher value of PCE weight. The cause for the high-performance of HK-PC is mainly due to the landscape of the Ishigami function that is better to be captured by PCE than the Kriging surrogate model.

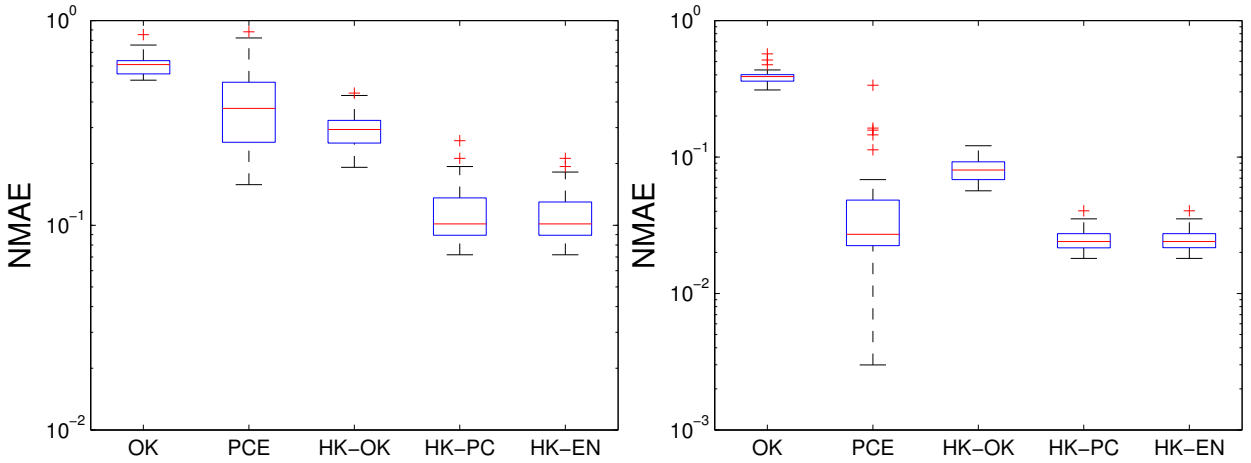

(a) $n_h = 30, n_l = 90$ (b) $n_h = 60, n_l = 180$

Figure 3: Boxplot of the $NMAE$ results on the Ishigami function from various surrogate model schemes.

Analysis of statistical moments is then performed. As can be seen in Figs. 4a and 5a, HK-PC and HK-EN have lower dispersion of $\mu(f(\boldsymbol{\xi}))$ and $\sigma(f(\boldsymbol{\xi}))$ than that of the others, as it was expected from the analysis of $NMAE$ results. In particular, the OK model has a very high error and high dispersion of $\sigma(f(\boldsymbol{\xi}))$ and $\mu(f(\boldsymbol{\xi}))$, but this can be improved by utilizing the HK framework. The more robust performance of HK-PC means that one has higher confidence in the results generated by HK if PCE is applied as the LF surrogate model. Nonetheless, one can rely on the ensemble of OK and PCE for the LF surrogate model if one is not sure which surrogate model type should be applied. When we observed the contribution of each surrogate model on the ensemble framework, it can be seen that the weight of PCE is near to one while the weight of Kriging is negligible. This means that there is no harm in applying the ensemble approach since it does not make the approximation worse.

We then analyze the result with a higher number of HF samples (i.e., $n_h = 60, n_l = 180$) as shown in Figs. 3b, 4b and 5b. The results with a higher number of HF samples is more complex than the previous one. Firstly, OK still found it very difficult to approximate the Ishigami function. We observe that HK-PC

and HK-EN produced surrogate models with better quality than that of HK-OK, which implies that HK with PCE as the LF surrogate model is still better than using Kriging for the Ishigami function. However, although the median $NMAE$ of HK-PC and HK-EN were lower than that of PCE, PCE has a significantly lower minimum $NMAE$ value of all. The reason why HK-PC and HK-EN cannot produce extremely accurate approximation on the Ishigami function with a high number of samples is because the main framework of the scheme itself is still Kriging. This implies that it is more difficult to approximate the Ishigami function with Kriging, in spite of the use of PCE for the LF surrogate model. Clearly, PCE is the best approximator here if seen from the viewpoint of achieving a very accurate value. Nonetheless, HK-PC and HK-EN were still more robust than PCE.

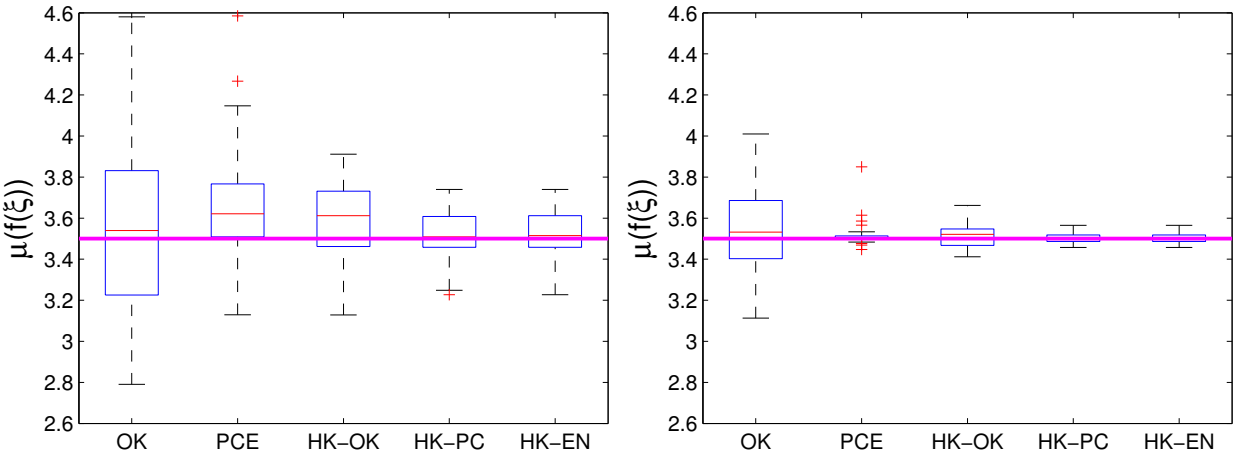

(a) $n_h = 30, n_l = 90$ (b) $n_h = 60, n_l = 180$

Figure 4: Boxplot of the $\mu(f(\boldsymbol{\xi}))$ on the Ishigami function from various surrogate model schemes (the magenta line is the analytical value).

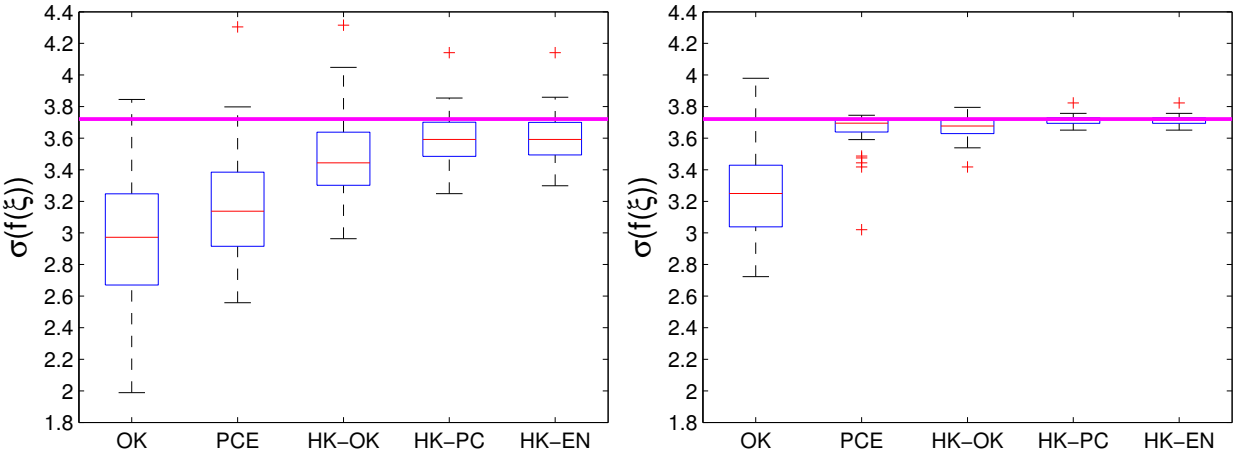

(a) $n_h = 30, n_l = 90$ (b) $n_h = 60, n_l = 180$

Figure 5: Boxplot of the $\sigma(f(\boldsymbol{\xi}))$ on the Ishigami function from various surrogate model schemes (the magenta line is the analytical value).

Based on the results from the Ishigami function, we observe that there is a potential to improve the performance of the original form of HK (i.e., HK-OK) for UQ purpose by approximating the LF function with other surrogate models than the OK. On the Ishigami function, which exhibits a complex trend, HK with PCE LF-model is superior to HK-OK from every aspect.

IV.B. Common Research Model in the Euler Flow

After the test on Ishigami function, we then demonstrate the usefulness of HK on CFD-based UQ problems. The first case is the UQ of CRM in the Euler flow in which the mesh is freely available online.[39] An open source CFD code of SU2 was used here to solve the Euler equation and to obtain the aerodynamic performance.[40] The same problem was studied in the context of UQ using MF-PCE.[27] The random inputs are the Mach number [Uniform, $0.82 - 0.84$], angle of attack [Uniform, $2^0 - 4^0$], and sideslip angle [Uniform, $0^0 - 2^0$], with the drag coefficient C_d as the random output of interest. Note that the use of the sideslip angle as a random variable is unrealistic here. However, our goal here is to demonstrate the capability of various MF methods for UQ applications; Hence, the use of the sideslip angle here is to made the problem more complex by having three random variables, while still being cheap to evaluate.

The HF and LF simulation for this case are the fully- and partially-converged simulation, with the number of maximum CFD iterations are roughly 600 and 100, respectively. The number of mesh elements used in this simulation is 38402. In this example, we used a low number of HF samples to better demonstrate the capability of HK for UQ. The number of HF samples was varied from 8 to 20 in a step of 2. For this problem, a constant scaling function was employed.

The LF training sample set was generated using LHS, where the HF sample set was then taken randomly from the corresponding LF sample set. We set $\boldsymbol{\mathcal{X}}_h \in \boldsymbol{\mathcal{X}}_l$ so we can make a fair comparison between HK and MF-PCE. Furthermore, we kept the number of LF samples to $n_h + 16$. For each combination of sample size and the UQ method, the computational experiment was repeated 40 times in order to obtain the median $NMAE$, $\mu(C_d)$, $\sigma(C_d)$ as shown in Fig. 7. With the cost of the LF evaluation roughly a sixth of the HF one, the total cost n_{tot} of the MF scheme is always $n_h + 2.66$ (adjusted to intersections of HF and LF samples that were evaluated together). Figure 6 shows an example of one realization of the CRM case together with the depiction of the surface mesh element. To calculate the $NMAE$ and reference values for statistical moments, a set of validation samples with $n_v = 800$ was utilized.

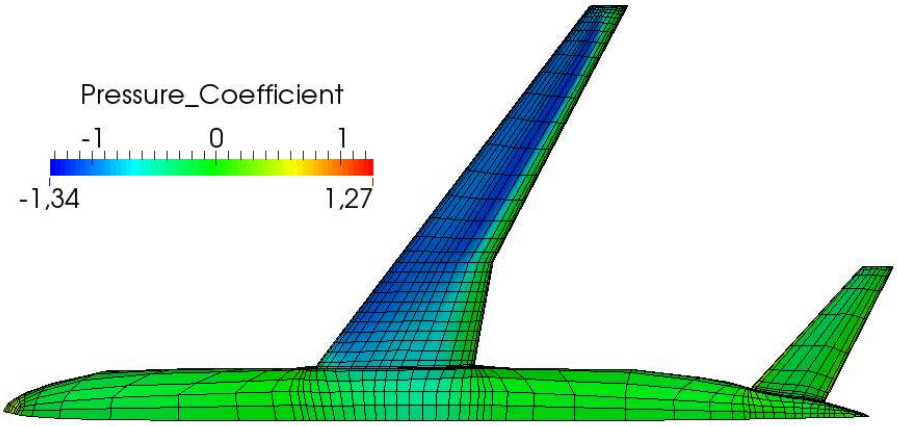

Figure 6: One realization of CRM case that depicts the pressure variation on the upper surface of the CRM.

The results show that the HK framework successfully reduced the approximation error compared to the single-fidelity schemes (see Fig. 7a), regardless of the HK scheme used for the approximation. There is no significant difference observed between the performance of all HK variants from the median $NMAE$ viewpoint. Moreover, all HK variants produced surrogate models with a lower median $NMAE$ compared to MF-PCE with additive (i.e., MF-PCE-A) and multiplicative correction (i.e., MF-PCE-M), which pointed out the advantage of applying the HK framework for MF approximation over the simple correction function as in MF-PCE. The worst performer here is obviously the single-fidelity PCE, with an obvious higher value of $NMAE$ compared to OK. It is also interesting to see here that for a similar value of n_{tot}, the $NMAE$ of MF-PCE is roughly similar with the single-fidelity OK. We can see that the enhancement of PCE with a MF formulation based on the correction function did not give significant improvement over the standard OK

method. The convergence of $\mu(c_d)$ and $\sigma(c_d)$ which are depicted in Figs. 7b and 7c, respectively, demonstrate that statistical moments generated by HK surrogate models were closer to 'true' values, which were obtained by using MCS with 800 samples, than that of single-fidelity approaches. On the other hand, MF-PCE needed more function evaluations to reach a sufficiently accurate approximation of statistical moments.

Fig. 8 shows the boxplot of results of $NMAE$, $\mu(C_d)$, and $\sigma(C_d)$ at $n_h = 20$. Note that the comparison between single-fidelity and MF methods is not entirely fair on this boxplot since the total computational cost is not the same for both approaches. In this boxplot, we can clearly see that, for all MF variants, all HK schemes consistently produced surrogate models with lower error than that of MF-PCE-A and MF-PCE-M. Observation of Figs 8b and 8c also reveals that the $\mu(C_d)$ and $\sigma(C_d)$ dispersion of HK with variation in the sampling set is much lower than that of MF-PCE-A and MF-PCE-M. This indicates the more consistent and robust performance of HK when subjected to the variation of sampling points. The HK-EN and HK-OK have a lower median $NMAE$ compared to HK-PC, although the difference is not significant.

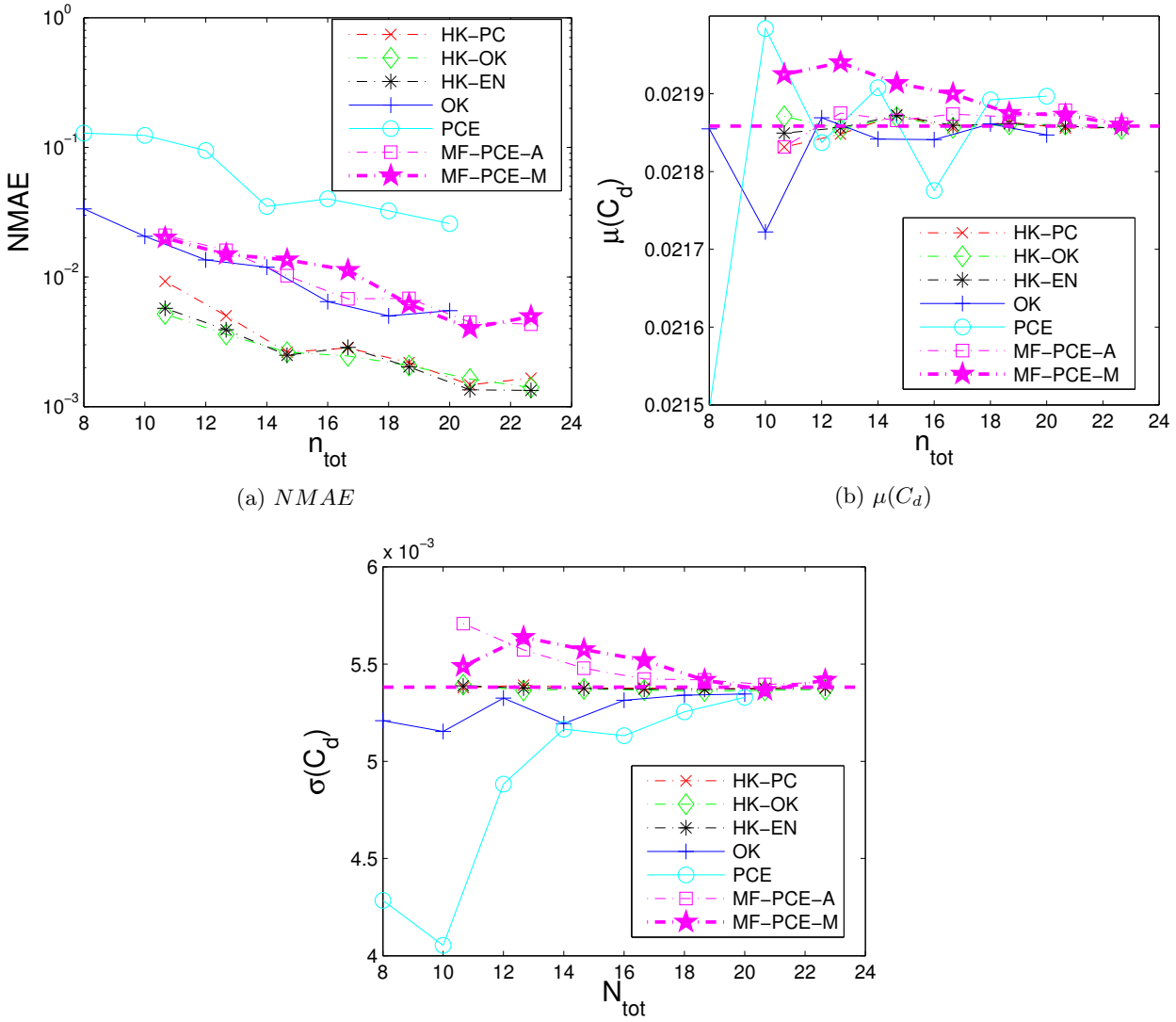

(a) $NMAE$

(b) $\mu(C_d)$

(c) $\sigma(C_d)$

Figure 7: Convergence of median results on the CRM problem (the straight magenta dashed line is the result from MCS).

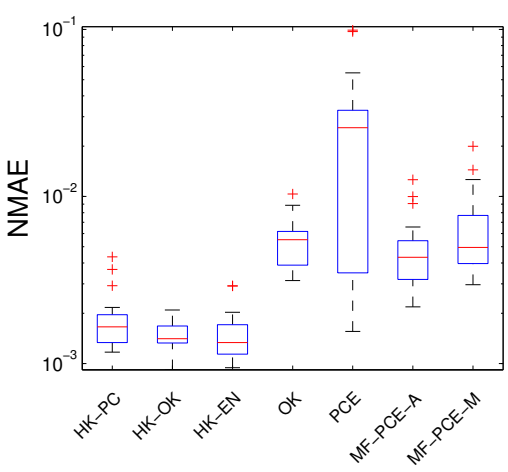

(a) $NMAE$

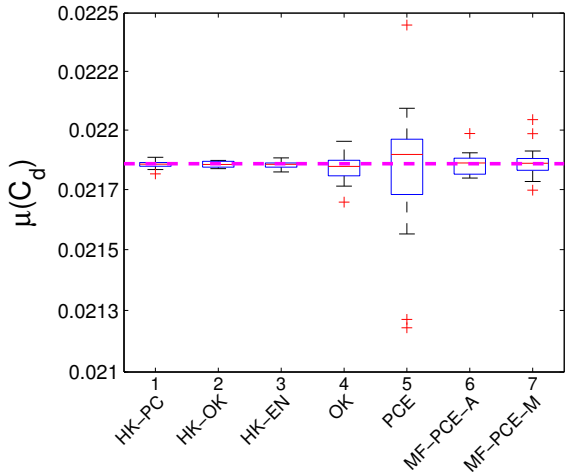

(b) $\mu(C_d)$

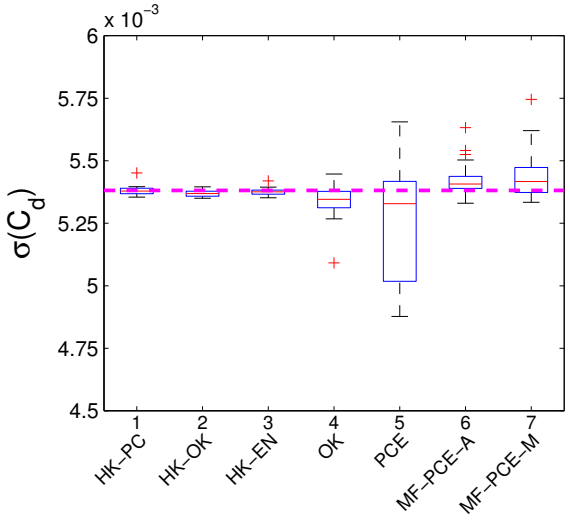

(c) $\sigma(C_d)$

Figure 8: Boxplot of the results with $n_h = 20$ on the CRM problem (the straight magenta dashed line is the result from MCS)

IV.C. RAE 2822 in the Euler flow

The second CFD-based case is the UQ of the RAE 2822 airfoil in the Euler flow. The high-fidelity simulation was solved through the Euler solver with 28414 mesh elements. Three types of coarse mesh were provided to support the MF UQ, where the fine and coarse meshes used for this case are shown in Fig. 9. The computational cost ratio, which is defined as the ratio between the high- and low-fidelity simulation, of the fine to coarse mesh with 7843, 3188, and 1983 mesh elements are roughly 4.4, 11.7, and 17.5, respectively. We denote the coarse mesh with 7843, 3188, and 1983 mesh elements as type A, B, and C, respectively, for the sake of brevity. For this problem, we set the Mach number and angle of attack as random variables with the distribution of $M \sim \text{Normal}[0.729,\ 0.005]$, and $AoA \sim \text{Normal}[2.31^0, 0.01^0]$, respectively, with L/D was set as the output of interest. The convergence of the median $NMAE$ for every UQ scheme was monitored in order to analyze the approximation quality of the surrogate model, where 200 independent validation samples were used to compute the $NMAE$. Performance comparison of all methodologies on this problem is better to be done by analyzing the $NMAE$, since it is difficult to do this task by comparing the convergence of statistical moments. We varied n_h from 6 to 15 in a step of 1, while the LF sample size was set to $n_h + 12$. The computational experiment was repeated 40 times with different set of LHS-generated samples.

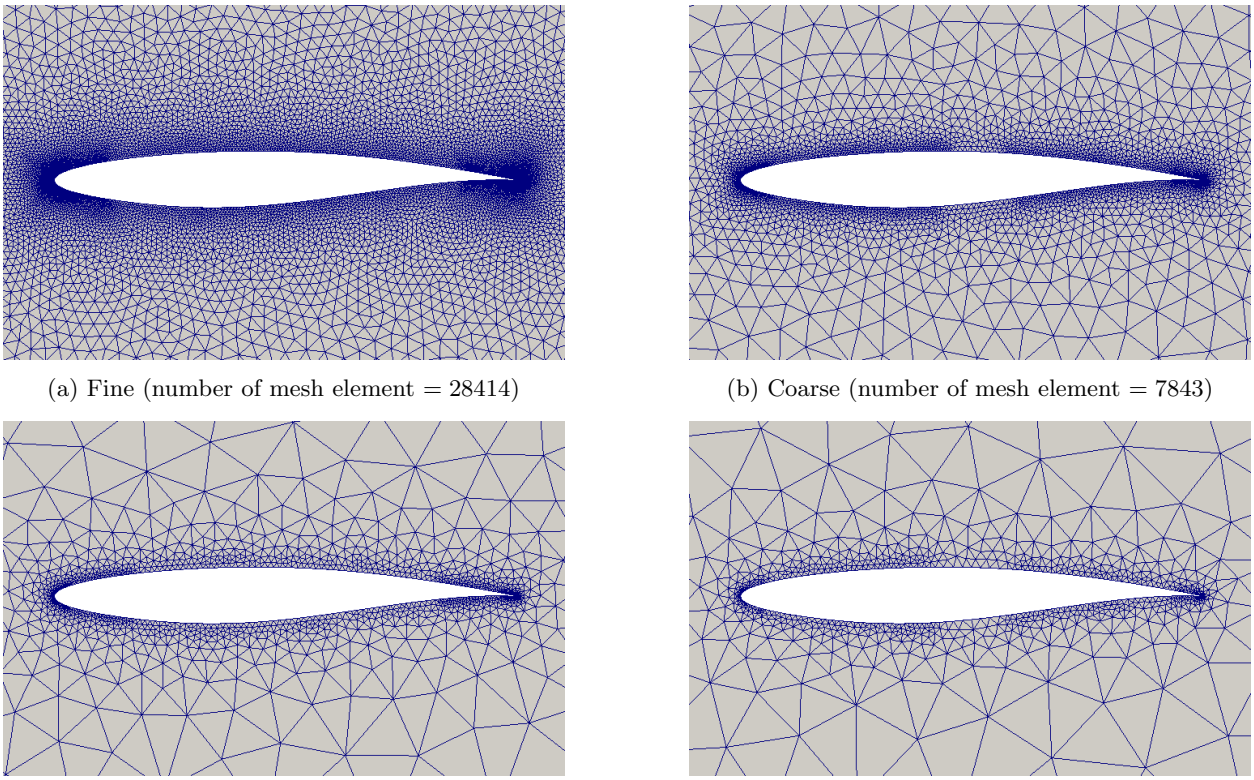

(a) Fine (number of mesh element = 28414)

(b) Coarse (number of mesh element = 7843)

(c) Coarse (number of mesh element = 3188)

(d) Coarse (number of mesh element = 1983)

Figure 9: Fine and coarse mesh used for the RAE 2822 Euler case.

For the inviscid RAE 2822 problem, we show the $NMAE$ convergence with both n_h and n_{tot} shown in the $x-$axis. The purpose of plotting the $NMAE$ as a function of n_h is to separate the analysis from the algorithmic and real-world efficiency viewpoint, where the former informs us whether the MF method works well or not without counting the actual cost of the LF simulation. On the other hand, comparing the algorithm's performance with the true actual cost allows us to analyze the efficiency of the algorithm in the real-world problem setting.

Firstly, we experimented with the standard form of HK (i.e., a constant regression multiplied by the LF function as the trend) with the $NMAE$ results shown in Figs. 10a and 10c. Analysis of Fig. 10a shows that only the type A LF mesh can properly assist the HK with constant scaling function so that it yields lower approximation error compared to OK. The coarsest mesh (type C) only made the approximation error worse while the type B coarse mesh did not yield any notable beneficial effect. When taking account the cost of

the LF simulation, we found that this MF strategy is not effective in decreasing the approximation error (see Fig. 10c). The standard form of HK with constant scaling function did not yield an advantage over the OK and PCE even with all three types of LF simulation and various LF surrogate models. Moreover, even the standard HF PCE is more efficient than that of OK and HK with constant scaling function here.

Increasing the order of scaling function to the first order polynomial yielded a beneficial effect as can be seen in Figs 10b and 10d. From the viewpoint of the effectiveness when the LF simulation cost is not counted, HK with first order scaling function was highly effective and showed clear benefit in reducing approximation error even when compared to HF PCE. It is also worth noting that all types of LF simulation were able to improve the accuracy of HK, as long as the first order scaling function was employed in the formulation. It is interesting to see that HK with first order scaling function and the coarsest mesh (i.e., type C) was the most efficient scheme here. This is because the MF scheme with the coarsest mesh as the LF sample typically yields a lower quality of approximation compared to the scheme with a less coarse mesh. Such typical trend is visible when a constant scaling function was employed but not with the first order scaling function. This indicates that the scaling function of HK with type C coarse mesh is probably less complex than that of other methods; However, more investigation is needed to further explore this issue. By taking account the cost of the LF simulation (see Fig. 10d), only the HK with the type C LF simulation delivered more efficiency than both HF approaches (i.e., OK and PCE). The fact that HK with a first order scaling function is highly efficient and the type C coarse mesh is the cheapest simulation in this problem, it is as expected that the combination of both is very effective as compared to OK with only a little extra computational cost. Regarding the type of the LF surrogate model, we observe no significant effect on the approximation quality when the type of the LF surrogate model was varied. This is particularly because there is no significant difference between the approximation quality of the LF surrogate model itself with the same sample size.

Comparison with MF-PCE approaches are shown in Fig. 11. Only the results from MF-PCE with multiplicative correction function is shown here since MF-PCE based on the additive correction function was less efficient than the multiplicative one for this problem. Furthermore, only the HK method with the ensemble of surrogate models is shown in order to avoid a too convoluted plot. We can see from these results that MF-PCE-M was not as efficient compared to HK with first order scaling function. Moreover, the HF and MF version of PCE performed roughly similar to each other, which means that the MF scheme with a simple correction function as in MF-PCE did not work well on this problem. MF-PCE-M only yielded lower $NMAE$ than its HF counterpart with $n_h = 6, 7$. However, it was not efficient when the true actual cost is considered.

Figure 12 shows the boxplot of the dispersion of $NMAE$ and statistical moments with $n_h = 15$. Here, only the results from the type C coarse mesh and the first order scaling function are shown since it is clear that this yielded the best possible approximation. Again, this comparison is not entirely fair since the total computational cost is different for HF and MF schemes. Firstly, Fig. 12a shows that HK-OK(C) and HK-EN(C) have a slightly lower median $NMAE$ than that of HK-PC(C), which shows the advantage of utilizing the ensemble approach although the difference is not so significant. The results for statistical moments as shown in Fig. 12b and 12c are encouraging as HK with the first order scaling function and the type C coarse mesh yielded the lowest dispersion of statistical moments. The MF-PCE-M scheme cannot advance further compared to its single-fidelity counterpart, as we can see that the dispersion of its statistical moments was still high.

V. Conclusions

In this paper, we studied the implementation and performance of the HK surrogate model for UQ purpose, especially for applications in CFD. We also enhanced the capability of HK by introducing PCE and the ensemble of PCE and OK to construct the LF surrogate model. This is possible due to the mathematical formulation of HK that allows the use of an arbitrary surrogate model for the LF function. Besides that, another enhancement that we proposed is to add polynomial scaling function to further improve the generalization capability of the HK framework.

We firstly investigated the capability of HK on the highly non-linear Ishigami test function. Results on the Ishigami function demonstrated the usefulness of HK to perform UQ, beyond its original use for optimization. On the Ishigami function, HK with PCE and the ensemble of surrogates as the LF surrogate model outperformed the standard HK method as indicated by the lower value of error and the lower dispersion of statistical moments over 50 different sample sets. This suggests that the original formulation of HK can be

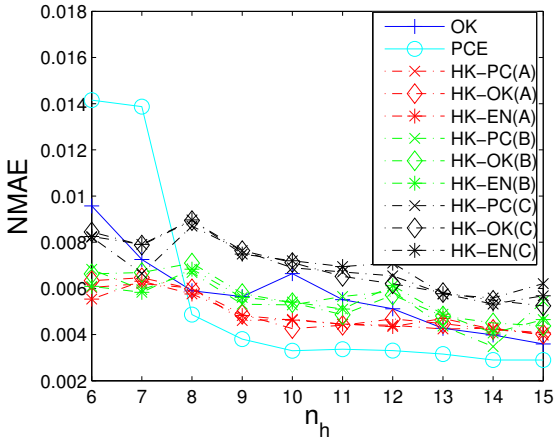

(a) HF simulation cost only, constant scaling function.

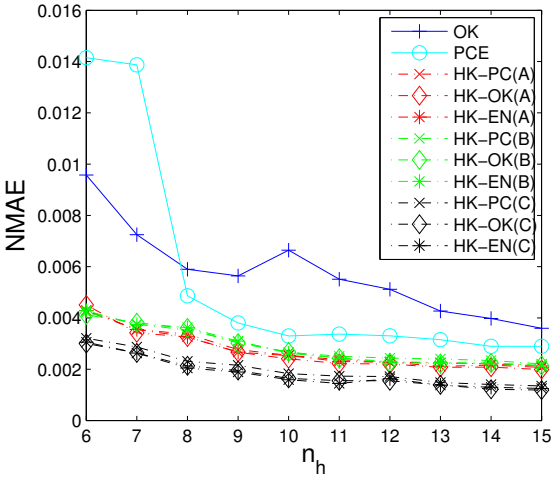

(b) HF simulation cost only, first order scaling function.

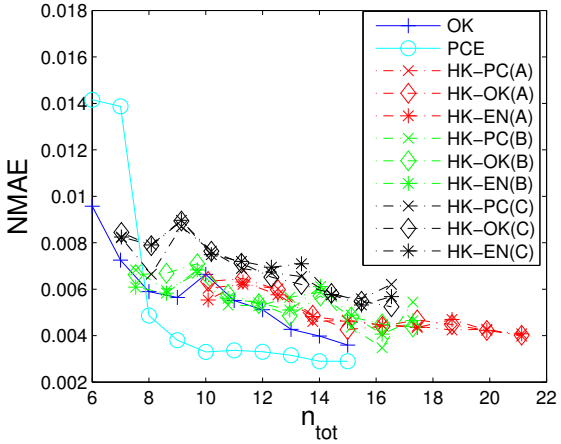

(c) Actual cost, constant scaling function.

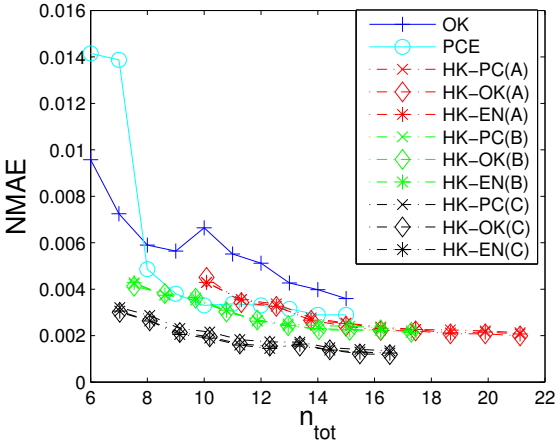

(d) Actual cost, first order scaling function.

Figure 10: Convergence of median $NMAE$ on the RAE 2822 Euler case.

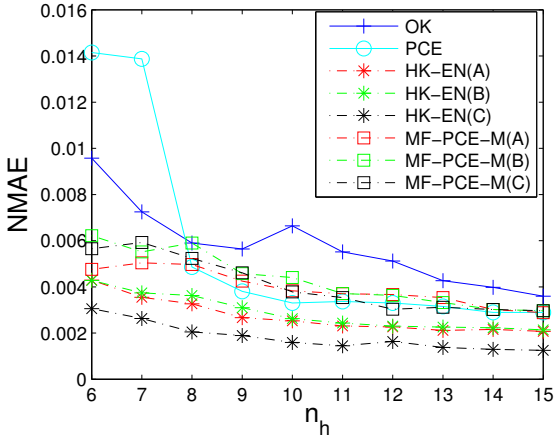

(a) HF simulation cost only

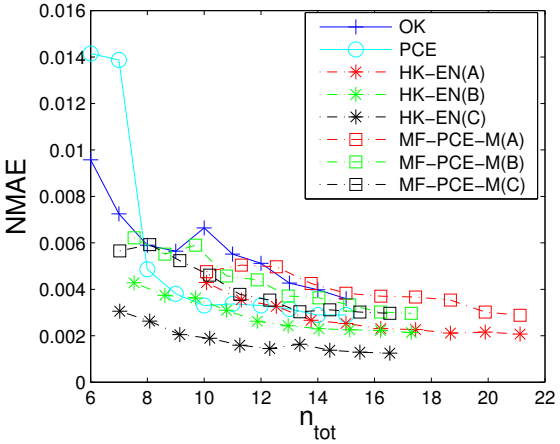

(b) Actual cost

Figure 11: Comparison of HK with the first order scaling function and MF-PCE on the RAE 2822 Euler case

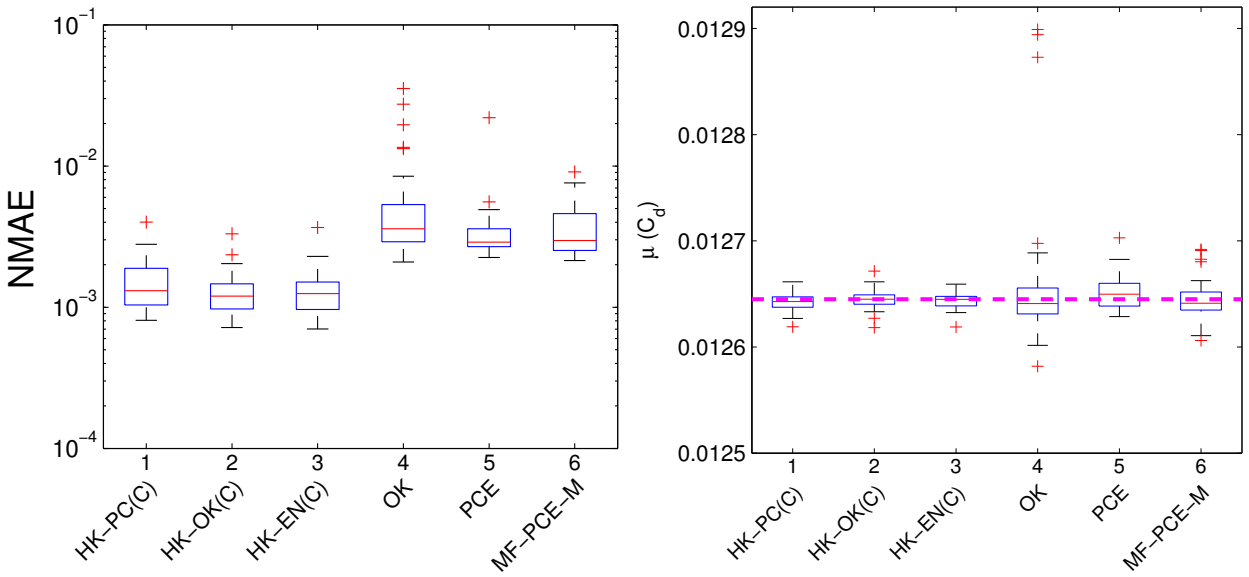

(a) $NMAE$

(b) $\mu(C_d)$

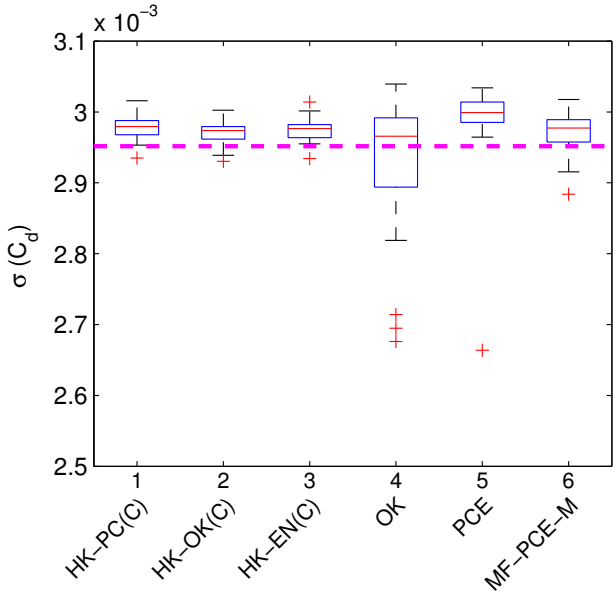

(c) $\sigma(C_d)$

Figure 12: Boxplot of results with $n_h = 15$ on the inviscid RAE 2822 problem, shown here is only HK with the first order scaling function (the straight magenta dashed line is the result from MCS)

further improved, especially for UQ purpose. Application to the UQ problem of CRM case in the Euler flow showed a good performance of the HK framework, outperforming single-fidelity OK, PCE, and MF-PCE. Using HK with a constant scaling function was not adequate to improve the effectiveness of HK in order to exceed the OK on the inviscid RAE 2822 problem. Instead, adding the first order polynomial to the scaling function greatly improved the generalization capability of HK on the inviscid RAE 2822 problem. The HK-EN showed more robust performance over the other methods on all test problems. When one cannot be sure which surrogate model to be used for the LF function, one can use the ensemble approach which ensures a good quality of the HK surrogate model.

There are several research avenues that could be pursued for the future work. Firstly, we found that a simple constant scaling function of the standard HK method might not perform well on some problems. Thus, research on the improvement of HK through the use of a more advanced scaling function or the method to properly choose the scaling function is needed. The methodology should also be investigated on more realistic (e.g. RANS equation) and higher-dimensional real-world problems (not just CFD-based problems) to further reveal the potential and peril of the HK method for solving UQ problem.

References

[1]Kbiob, D., "A statistical approach to some basic mine valuation problems on the Witwatersrand," *Journal of Chemical, Metallurgical, and Mining Society of South Africa*, 1951.

[2]Lesh, F. H., "Multi-dimensional least-squares polynomial curve fitting," *Communications of the ACM*, Vol. 2, No. 9, 1959, pp. 29–30.

[3]Buhmann, M. D., "Radial basis functions," *Acta Numerica 2000*, Vol. 9, 2000, pp. 1–38.

[4]Ghiocel, D. M. and Ghanem, R. G., "Stochastic finite-element analysis of seismic soil-structure interaction," *Journal of Engineering Mechanics*, Vol. 128, No. 1, 2002, pp. 66–77.

[5]Berveiller, M., Sudret, B., and Lemaire, M., "Stochastic finite element: a non intrusive approach by regression," *European Journal of Computational Mechanics/Revue Européenne de Mécanique Numérique*, Vol. 15, No. 1-3, 2006, pp. 81–92.

[6]Smola, A. and Vapnik, V., "Support vector regression machines," *Advances in neural information processing systems*, Vol. 9, 1997, pp. 155–161.

[7]Shafer, G. et al., *A mathematical theory of evidence*, Vol. 1, Princeton university press Princeton, 1976.

[8]Lewis, R. M. and Huyse, L., "Aerodynamic shape optimization of two-dimensional airfoils under uncertain conditions," Tech. rep., DTIC Document, 2001.

[9]Dodson, M. and Parks, G. T., "Robust aerodynamic design optimization using polynomial chaos," *Journal of Aircraft*, Vol. 46, No. 2, 2009, pp. 635–646.

[10]Wang, X., Hirsch, C., Liu, Z., Kang, S., and Lacor, C., "Uncertainty-based robust aerodynamic optimization of rotor blades," *International Journal for Numerical Methods in Engineering*, Vol. 94, No. 2, 2013, pp. 111–127.

[11]Sudret, B., "Global sensitivity analysis using polynomial chaos expansions," *Reliability Engineering & System Safety*, Vol. 93, No. 7, 2008, pp. 964–979.

[12]Crestaux, T., Le Maıˆtre, O., and Martinez, J.-M., "Polynomial chaos expansion for sensitivity analysis," *Reliability Engineering & System Safety*, Vol. 94, No. 7, 2009, pp. 1161–1172.

[13]Xiu, D. and Karniadakis, G. E., "Modeling uncertainty in flow simulations via generalized polynomial chaos," *Journal of computational physics*, Vol. 187, No. 1, 2003, pp. 137–167.

[14]Mathelin, L., Hussaini, M. Y., Zang, T. A., and Bataille, F., "Uncertainty propagation for a turbulent, compressible nozzle flow using stochastic methods," *AIAA journal*, Vol. 42, No. 8, 2004, pp. 1669–1676.

[15]Ghisu, T., Parks, G. T., Jarrett, J. P., and Clarkson, P. J., "Adaptive polynomial chaos for gas turbine compression systems performance analysis," *AIAA Journal*, Vol. 48, No. 6, 2010, pp. 1156–1170.

[16]Simon, F., Guillen, P., Sagaut, P., and Lucor, D., "A gPC-based approach to uncertain transonic aerodynamics," *Computer Methods in Applied Mechanics and Engineering*, Vol. 199, No. 17, 2010, pp. 1091–1099.

[17]Hosder, S., Walters, R. W., and Balch, M., "Point-collocation nonintrusive polynomial chaos method for stochastic computational fluid dynamics," *AIAA journal*, Vol. 48, No. 12, 2010, pp. 2721–2730.

[18]Blatman, G. and Sudret, B., "Adaptive sparse polynomial chaos expansion based on least angle regression," *Journal of Computational Physics*, Vol. 230, No. 6, 2011, pp. 2345–2367.

[19]Shimoyama, K., Kawai, S., and Alonso, J. J., "Dynamic adaptive sampling based on Kriging surrogate models for efficient uncertainty quantification," *15th AIAA Non-Deterministic Approaches Conference*, 2013, pp. 2013–1470.

[20]Kawai, S. and Shimoyama, K., "Kriging-model-based uncertainty quantification in computational fluid dynamics," *32nd AIAA Applied Aerodynamics Conference*, 2013.

[21]Dwight, R. P. and Han, Z.-H., "Efficient uncertainty quantification using gradient-enhanced kriging," *AIAA paper*, Vol. 2276, 2009, pp. 2009.

[22]Lockwood, B. A. and Anitescu, M., "Gradient-enhanced universal kriging for uncertainty propagation," *Nuclear Science and Engineering*, Vol. 170, No. 2, 2012, pp. 168–195.

[23]De Baar, J., Scholcz, T. P., Verhoosel, C. V., Dwight, R. P., van Zuijlen, A. H., and Bijl, H., "Efficient uncertainty quantification with gradient-enhanced kriging: Applications in fsi," *Eccomas Vienna*, 2012.

[24]Dwight, R. P., Witteveen, J. A., and Bijl, H., "Adaptive uncertainty quantification for computational fluid dynamics," *Uncertainty Quantification in Computational Fluid Dynamics*, Springer, 2013, pp. 151–191.

[25]Owen, N., Challenor, P., Menon, P., and Bennani, S., "Comparison of surrogate-based uncertainty quantification methods for computationally expensive simulators," *arXiv preprint arXiv:1511.00926*, 2015.

[26]Ng, L. W.-T. and Eldred, M., "Multifidelity uncertainty quantification using nonintrusive polynomial chaos and stochastic collocation," *Proceedings of the 14th AIAA Non-Deterministic Approaches Conference, number AIAA-2012-1852, Honolulu, HI*, Vol. 43, 2012.

[27]Palar, P. S., Tsuchiya, T., and Parks, G. T., "Multi-fidelity non-intrusive polynomial chaos based on regression," *Computer Methods in Applied Mechanics and Engineering*, Vol. 305, 2016, pp. 579–606.

[28]Padrón, A. S., Alonso, J. J., and Eldred, M. S., "Multi-fidelity Methods in Aerodynamic Robust Optimization," *18th AIAA Non-Deterministic Approaches Conference*, 2016, p. 0680.

[29]Kennedy, M. C. and O'Hagan, A., "Predicting the output from a complex computer code when fast approximations are available," *Biometrika*, Vol. 87, No. 1, 2000, pp. 1–13.

[30]de Baar, J., Roberts, S., Dwight, R., and Mallol, B., "Uncertainty quantification for a sailing yacht hull, using multi-fidelity kriging," *Computers & Fluids*, Vol. 123, 2015, pp. 185–201.

[31]Le Gratiet, L., Cannamela, C., and Iooss, B., "A Bayesian approach for global sensitivity analysis of (multifidelity) computer codes," *SIAM/ASA Journal on Uncertainty Quantification*, Vol. 2, No. 1, 2014, pp. 336–363.

[32]Han, Z.-H. and Görtz, S., "Hierarchical Kriging model for variable-fidelity surrogate modeling," *AIAA journal*, Vol. 50, No. 9, 2012, pp. 1885–1896.

[33]Han, Z.-H., Görtz, S., and Zimmermann, R., "Improving variable-fidelity surrogate modeling via gradient-enhanced kriging and a generalized hybrid bridge function," *Aerospace Science and Technology*, Vol. 25, No. 1, 2013, pp. 177–189.

[34]Goel, T., Haftka, R. T., Shyy, W., and Queipo, N. V., "Ensemble of surrogates," *Structural and Multidisciplinary Optimization*, Vol. 33, No. 3, 2007, pp. 199–216.

[35]Acar, E. and Rais-Rohani, M., "Ensemble of metamodels with optimized weight factors," *Structural and Multidisciplinary Optimization*, Vol. 37, No. 3, 2009, pp. 279–294.

[36]Dubrule, O., "Cross validation of kriging in a unique neighborhood," *Journal of the International Association for Mathematical Geology*, Vol. 15, No. 6, 1983, pp. 687–699.

[37]Toal, D. J., "Some considerations regarding the use of multi-fidelity Kriging in the construction of surrogate models," *Structural and Multidisciplinary Optimization*, Vol. 51, No. 6, 2015, pp. 1223–1245.

[38]Ishigami, T. and Homma, T., "An importance quantification technique in uncertainty analysis for computer models," *Uncertainty Modeling and Analysis, 1990. Proceedings., First International Symposium on*, IEEE, 1990, pp. 398–403.

[39]"Test cases for SU2," 2015, [Online; accessed 22-June-2015].

[40]Palacios, F., Colonno, M. R., Aranake, A. C., Campos, A., Copeland, S. R., Economon, T. D., Lonkar, A. K., Lukaczyk, T. W., Taylor, T. W., and Alonso, J. J., "Stanford University Unstructured (SU2): An open-source integrated computational environment for multi-physics simulation and design," *AIAA Paper*, Vol. 287, 2013, pp. 2013.